RAA 2016 Vol. **16** No. **7**, 115 (10pp) doi: 10.1088/1674–4527/16/7/115
http://www.raa-journal.org *http://iopscience.iop.org/raa*

***R**esearch in*
***A**stronomy and*
***A**strophysics*

Study of the continuum removal method for the Moon Mineralogy Mapper (M^3) and its application to Mare Humorum and Mare Nubium

Xun-Yu Zhang[1], Zi-Yuan Ouyang[2], Xiao-Meng Zhang[3], Yuan Chen[3], Xiao Tang[3,4], Ao-Ao Xu[1], Ze-Sheng Tang[1] and Yun-Zhao Wu[3]

[1] Space Science Institute, Macau University of Science and Technology, Macau 00853, China
[2] National Astronomical Observatories, Chinese Academy of Sciences, Beijing 100012, China
[3] School of Geographic and Oceanographic Sciences, Nanjing University, Nanjing 210023, China; *wu@nju.edu.cn*
[4] Key Laboratory of Planetary Sciences, Chinese Academy of Sciences, Nanjing 210008, China

Received 2015 November 23; accepted 2016 March 19

Abstract The absorption band center of visible and near infrared reflectance spectra is a key spectral parameter for lunar mineralogical studies, especially for the mafic minerals (olivine and pyroxene) of mare basalts, which have two obvious absorption bands at 1000 nm (Band I) and 2000 nm (Band II). Removal of the continuum from spectra, which was developed by Clark and Roush and used to isolate the particular absorption feature, is necessary to estimate this parameter. The Moon Mineralogy Mapper (M^3) data are widely used for lunar mineral identification. However, M^3 data show a residual thermal effect, which interferes with the continuum removal, and systematic differences exist among optical data taken during different optical periods. This study investigated a suitable continuum removal method and compared the difference between two sets of M^3 data taken during different optical periods, Optical Period 1B (OP1B) and Optical Period 2A (OP2A). Two programs for continuum removal are reported in this paper. Generally, a program respectively constructs two straight lines across Band I and Band II to remove the continuum, which is recommended for locating band centers, because it can find the same Band I center with different right endpoints. The optimal right endpoint for continuum removal is mainly dominated by two optical period data at approximately 2480 and 2560 nm for OP1B and OP2A data, respectively. The band center values derived from OP1B data are smaller than those derived from OP2A data in Band I but larger in Band II, especially for the spectra using longer right endpoints (>2600 nm). This may be due to the spectral slopes of OP1B data being steeper than those of OP2A data in Band I but gentler in Band II. These results were applied to Mare Humorum and Mare Nubium, and the measurements were found to mainly vary from intermediate- to high-Ca pyroxene.

Key words: techniques: spectroscopic — methods: data analysis — instrumentation: spectrographs

1 INTRODUCTION

Mare basalts are the primary rock type within maria (Pieters et al. 1980; Staid & Pieters 2001). They are the key to understanding the formation and evolution of the Moon (Staid et al. 2011). The most common minerals of mare basalts are pyroxene, olivine, plagioclase and ilmenite (Staid & Pieters 2001; Lucey 2004). The reflectance spectra within visible and near infrared wavelengths (400-2500 nm) are sensitive to these minerals (Lucey 2004; Staid et al. 2011). The spectrum of pyroxene has two absorption bands at 1000 nm (Band I) and 2000 nm (Band II) (Adams 1975; Cloutis 1985). The reflectance spectrum of olivine has broad Band I absorption, but lacks Band II absorption (Adams 1975; Burns 1993). Plagioclase feldspar and Fe-rich glass also show Band I absorption but without a significant Band II feature. However, weak plagioclase absorptions are not visible in the presence of mafic minerals (Crown & Pieters 1987). It is unlikely that Fe-rich glass produces olivine-like strong absorption in the spectra extracted from fresh craters (Pieters et al. 1980). The absorption band center is the key spectral parameter for mineral identification of mare basalts, especially for olivine and pyroxene, which have diagnostic absorptions that vary with composition (Adams 1975; Burns 1993; Cloutis 1985).

To assess the absorption band centers and outline the absorption features, it is necessary to remove the continuum from spectra. The convex hull method, developed by Clark & Roush (1984), is widely used for continuum removal from reflectance spectra. It uses a convex hull fit over the top of a spectrum with straight-line segments that connect local spectral maxima to construct the continuum. Continuum removal is defined as the ratio of the reflectance value of the spectrum to the continuum value of

the corresponding band. The result is a relative reflectance called the continuum-removed reflectance. Because the first and last spectral data values are on the hull, the values of the first and last bands are equal to 1 in the output continuum-removed reflectance file.

The Moon Mineralogy Mapper (M^3), an imaging spectrometer that is a guest instrument onboard the Indian Chandrayaan-1 mission (Pieters et al. 2009), has been widely used for lunar mineral identification (Staid et al. 2011; Kusuma et al. 2012). Unfortunately, M^3 data have a residual thermal effect (Clark et al. 2011), where the reflectance increases continuously at long wavelengths (> 2000 nm), which interferes with continuum removal. Previous studies cut off the right endpoint of spectra at different positions during continuum removal, such as 2500 nm (e.g., Kusuma et al. 2012), 2600 nm (Klima et al. 2011) or 3000 nm (Varatharajan et al. 2014). These papers did not provide sufficient reasons for the assignments of the right endpoint or compare the band centers derived from these methods. Moreover, these studies only used one set of sub-Optical Period M^3 data (there are a total of five sub-Optical Periods), but the band centers vary in different optical periods because of the existence of systematic bias (Wu et al. 2015; Isaacson et al. 2012) in the reflectance. Wu et al. (2015) used large amounts of data from Mare Imbrium to explore the continuum removal method for M^3 data by changing the right endpoints and compared the band center values between Optical Period 1B (OP1B) data and Optical Period 2A (OP2A) data. They found that the band center values between the two optical period data are related to the continuum slopes and suggested that 2497 nm is the right endpoint for continuum removal for both OP1B and OP2A data. However, their research area is limited to only Mare Imbrium, and whether their conclusions can be applied to other areas or not is unknown. Moreover, during their continuum removal, the convex hull method was used across the entire wavelength range. They did not perform continuum removal for Band I and Band II separately.

In summary, it is necessary to use more samples and different areas for further research and perform continuum removal for Band I and Band II separately. The purpose of this paper is to determine a more suitable continuum removal method for OP1B and OP2A M^3 data. A comparison of the spectral features between OP1B and OP2A data was applied to both Mare Humorum and Mare Nubium.

2 DATA AND METHOD

2.1 M^3 Data

The Chandrayaan-1 mission was launched on 2008 October 22 and finished its mission in August of 2009. M^3 imaged the Moon in two modes: global mode and target mode (Green et al. 2011). It operated in the spectral channels from 430 to 3000 nm. For target mode, M^3 acquired images with a spatial resolution of 70 m/pix in 260 channels. In global mode, it acquired images with 140×140 m or 140×280 m per pixel in 85 channels (Pieters et al. 2009). The global data have five sets of sub-Optical Periods (OP): OP1A, OP1B, OP2A, OP2B and OP2C. During its ten-month nominal mission in lunar polar orbit, it observed more than 95% of the Moon in global mode and obtained a small number of images in target mode (Boardman et al. 2011). Initial global mode data coverage of Mare Humorum and Mare Nubium during OP1B and OP2A were incomplete (Fig. 1). This paper focuses mainly on the spectra (acquired in global mode) in the regions of Mare Humorum and Mare Nubium covered by both OP1B and OP2A data.

2.2 Spectral Extraction

Space weathering weakens the spectral absorptions of lunar mafic minerals (McCord & Adams 1973; Pieters et al. 2000). To accurately characterize the spectral features, fresh craters with bright rays were chosen to extract the spectra. The spectra of OP1B and OP2A data were extracted from the same crater for comparison. Because the solar angles of OP1B and OP2A data are diffident (OP1B data were collected in the lunar morning and OP2A data were collected in the lunar afternoon), the spectra were extracted on different sides of the craters. The spectra of the OP1B data were extracted from the west side of the crater walls (rims), and those of the OP2A data were from the east side of the crater walls (rims). The thicknesses of mare basalt layers are generally thin (Hiesinger et al. 2000, 2003) and large craters may excavate the upper flows and expose the lower basalts, which lead the crater walls (rims) to have a different composition. It is helpful to reduce this influence by extracting the spectra from small craters. However, for craters smaller than the spatial resolution of M^3 data, the spectra are not only from fresh rocks but also from mature soils and shadows. A fresh crater with a diameter of about 500 m is optimal to not only distinguish the wall from a shadow but also represent the top unit.

Hence, following the method suggested in Wu et al. (2015), in this study most spectra were extracted from resolvable small fresh craters (about 500 m) and from only one pixel to reduce spectral mixing. This pixel had the highest-quality spectrum among all the pixels covering the crater. For a few craters with low signal-to-noise ratio spectra, the average spectra were represented by 2×2 pixels. Figure 2 shows an example of a small fresh crater from which spectra were extracted. The spectra of a fresh crater and a mature crater are also presented for comparison. After careful manual selection, 257 small fresh craters (75 craters from Mare Humorum and 182 craters from Mare Nubium) were selected to perform the following analysis (Fig. 1).

2.3 Continuum Removal

The spectra were first smoothed by B spline smoothing before continuum removal (see Fig. 3) to reduce the effect of noise (Wu et al. 2015). Figure 3 presents an example of the

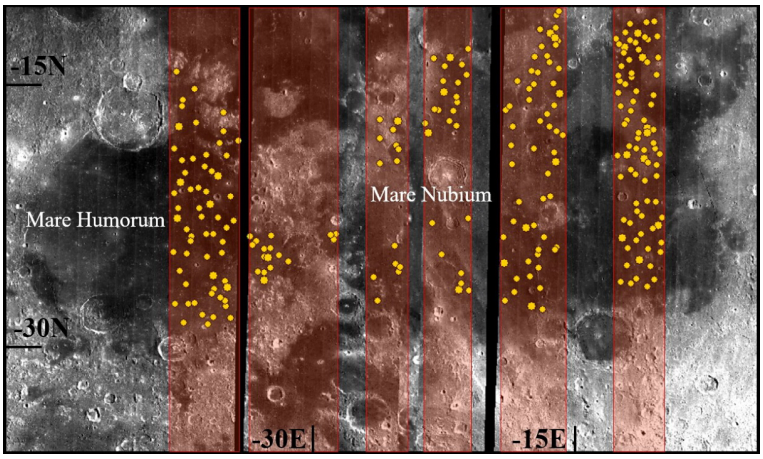

Fig. 1 Map of the maria studied in this paper. Mare Humorum is on the left side and Mare Nubium is on the right side. The base map is a mosaic of M^3 images (OP1B data: 1508 nm). The yellow spots mark the fresh craters collected in this study. The red boxes represent areas covered by both OP1B and OP2A data.

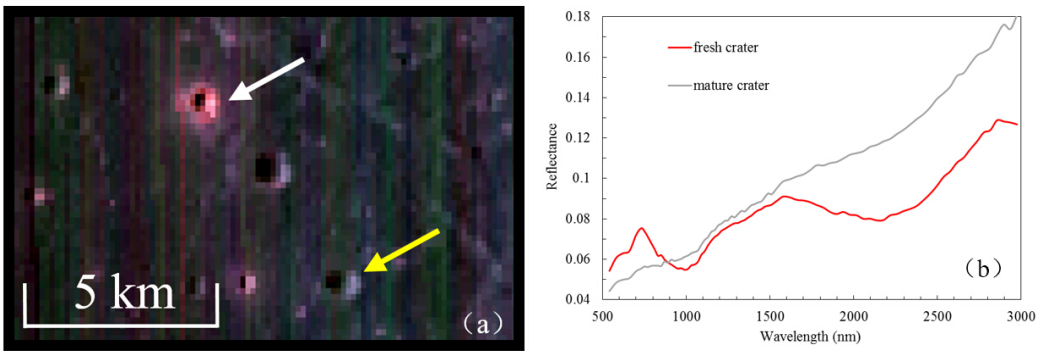

Fig. 2 Comparison of a small fresh crater and a mature crater. (a) The base map is an M^3 color composite image (OP2A data: red-750 nm, green-950 nm, blue-1500 nm). The white arrow marks the fresh crater with a bright ray. The yellow arrow shows the mature crater. (b) The spectra extracted from the two craters.

convex hull method applied to the spectra of mare basalts. In the convex hull method, Band I absorption typically has two inflection points around 750 and 1500 nm. The straight-line segment across Band II absorption usually connects the left shoulder (around 1500 nm) with the right endpoint, which is determined by researchers, because the residual thermal effect of M^3 data increases the reflectance at long wavelengths ($>$ 2000 nm). In some cases, as the right endpoint moves to longer wavelengths during continuum removal, there is no tangent point around 1500 nm between Band I and Band II. Thus, there is only one line segment across both Band I and Band II for the convex hull method, as shown by the red dashed line in Figure 4. This variation affects the band centers.

Hence, two programs that remove the continuum were used to study the band center variation. One applied the convex hull method to both Band I and Band II of the spectra for continuum removal (Program I) once in ENVI (Fig. 4), which is similar to the method used by Wu et al. (2015). The other separately constructed two straight lines across Band I and Band II to remove the continuum individually (Program II). For Program II, the straight line was tangent to the spectra on the left and right shoulder of the target absorption band. As Figure 4 illustrates, for Band I, the tangent points of the line are around 750 and 1500 nm. For Band II, they usually appear around 1500 nm and the right endpoint position.

2.4 Spectral Parameters

The spectral resolution of M^3 data is about 20 nm around Band I and 40 nm around Band II. This is not precise enough for estimating the band centers by choosing an individual M^3 channel. Following Wu et al. (2015), a sixth order polynomial curve was fitted at the quarter bottom of the continuum-removed absorption band to derive the band center. The wavelength (with resolution higher than 0.01 nm) with the smallest continuum removed reflectance was considered to be the most accurate band center (see Fig. 4). This band center estimation method was applied to both Band I and Band II. As discussed above, different right endpoints affect the band centers. To analyze this influence for both Program I and Program II, the right endpoint of the spectra was tested at seven wavelengths: 2457 nm (Point I), 2497 nm (Point II), 2536 nm (Point III),

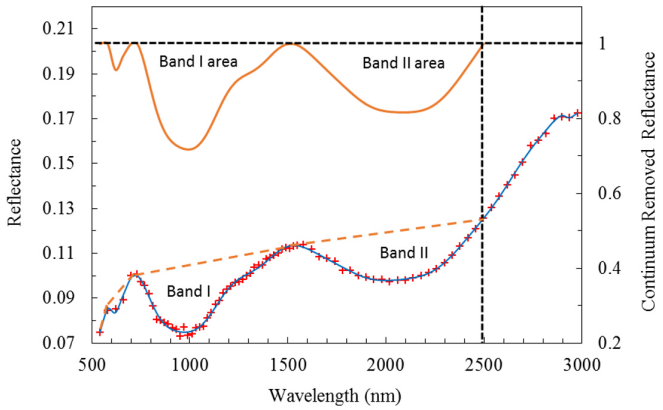

Fig. 3 Example of continuum removal (the convex hull method) and denoising for the spectrum truncated at 2497 nm. Red "+" points are the original M^3 reflectance data. The blue line depicts the spectrum after smoothing. The orange dashed line represents the straight-line segments of the convex hull, and the orange solid line represents the spectrum after continuum removal. The black dashed lines indicate the right endpoint position (*vertical*) and where the continuum removed reflectance equals 1 (*horizontal*).

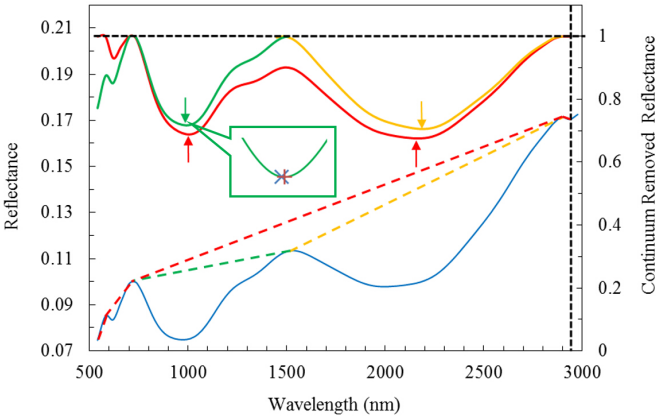

Fig. 4 Illustration of Program I and Program II for continuum removal (the right endpoint at 2936 nm). The arrows show the locations of absorption band centers. The blue cross shows the channel of M^3 data with minimum continuum removed reflectance. The red cross presents a more precise band center introduced by Wu et al. (2015). The red dashed line and solid line represent the straight-line segments used in Program I and the continuum-removed result, respectively. The green and orange dashed lines denote the tangent lines used in Program II across Band I and Band II respectively. The green and orange solid lines represent the continuum-removed results using Program II for Band I and Band II respectively. The black dashed lines indicate the right endpoint position (*vertical*) and where the continuum removed reflectance equals 1 (*horizontal*).

2576 nm (Point IV), 2616 nm (Point V), 2776 nm (Point VI) and 2936 nm (Point VII).

In the plot of Band II center versus Band I center, which is widely used to compare the pyroxene and olivine, the curve of a quadratic equation was fitted (Fig. 5) with the data for natural orthopyroxenes and clinopyroxenes (Adams 1974; Cloutis & Gaffey 1991). It represents the trend of natural pyroxenes and was used to determine the optimal right endpoints of spectra for continuum removal. As mentioned above, the spectra of mare basalt, which were extracted from the fresh crater, are mainly sensitive to the composition of olivine and pyroxene. In the olivine-pyroxene mixtures, Band II is mainly sensitive to the pyroxene abundance (orthopyroxene and clinopyroxene), while Band I is dependent on the relative abundances of olivine and pyroxene (Cloutis et al. 1986). The Band I center will slightly move to a longer wavelength due to the presence of olivine. Natural pyroxene is not an ideal target for comparing the band centers of mare basalts because some deviations exist. However, the types of mare basalts sampled by Apollo missions were limited, and although Mare Humorum and Mare Nubium were considered to be pyroxene-dominated regions in previous studies (Pieters 1978; Lucey 2004; Staid et al. 2011), some deviations still exist. The band centers of natural orthopyroxenes and clinopyroxenes, which are widely used for lunar mineral identification (Klima et al. 2007; Varatharajan et al. 2014), provide an approximate trend of the Band I center and Band II center to study the behaviors of the band centers derived from spectra with different right points, for OP1B and OP2A data. As Figure 5 shows, for the spectra using the same program for continuum removal, the band centers of these measurements varied for different right endpoints, which also changed the average distances

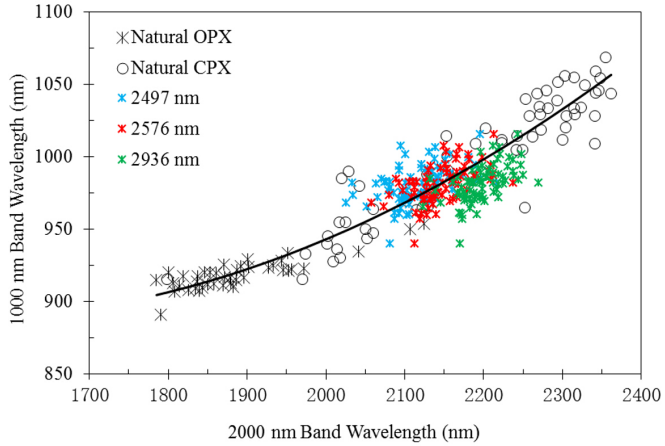

Fig. 5 The plot of Band II center versus Band I center. Measurements of the craters extracted from Mare Humorum (OP2A data), which used Program II and different right endpoints (2497, 2576 and 2936 nm) for continuum removal, are presented for comparison with natural pyroxenes measured by Adams (1974) and modified by Cloutis & Gaffey (1991). The black line represents the fitting curve of natural pyroxenes. OPX means orthopyroxene and CPX means clinopyroxene.

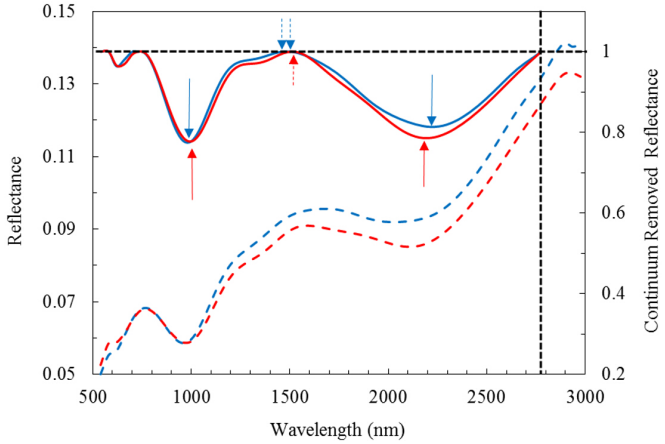

Fig. 6 Illustration of the OP1B and OP2A spectra extracted from the same small fresh crater (using Program I for continuum removal and Point VI as the right endpoint). The blue dashed line and blue solid line display the spectrum of the OP1B data and the continuum-removed result, respectively. The red dashed line and red solid line represent the spectrum of the OP2A data and the continuum-removed result respectively. The solid arrows show the locations of the band centers. The dashed arrows display the tangent points of the continuums around 1500 nm. The black dashed lines indicate the right endpoint position (*vertical*) and where the continuum removed reflectance equals 1 (*horizontal*).

(from the measurement position to the fitting curve in the band center plot). The measurements with the shortest average distance are considered to be the best fit of the natural pyroxenes, which means the corresponding right endpoint (between 2457 to 2936 nm) of these spectra used for continuum removal is considered to be the optimal right endpoint.

In the olivine-pyroxene mixtures, Band I is highly influenced by multiple overlapping absorptions which make the interpretations difficult. The relative absorption area ratio of Band II to Band I (Band Area Ratio, i.e., BAR) is a useful spectral parameter for estimating the relative abundances of pyroxene and olivine (Cloutis et al. 1986). BAR is inversely proportional to the abundance of olivine for basalts, but increases linearly when the pyroxene abundance increases (Cloutis et al. 1986). Cloutis et al. (1986) and Gaffey et al. (1993) introduced the plot of BAR versus Band I center to study the spectral behavior of olivine, clinopyroxene and orthopyroxene mixtures. Although Cloutis et al. (1986) and Gaffey et al. (1993) used it for asteroidal studies, for the olivine-pyroxene mixtures, the BAR value is inversely proportional to the abundance of olivine, but increases linearly when the pyroxene abundance increases. Considering that the spectra of mare basalt are mainly sensitive to olivine and pyroxene, they can be used to study the relative content of olivine and pyroxene in mare basalts. To estimate the band area, Point II (2497 nm) was used as the right endpoints of spectra for both OP1B and OP2A data. An example of the band area estimation is presented in Figure 3, which shows the integrated area of the continuum-removed reflectance and the $y = 1$ line.

3 RESULTS AND DISCUSSION

3.1 Comparison between the Two Continuum Removal Programs

In the situation where the line segment used in Program I has at least one inflection point around 1500 nm in the spectrum, continuum removal using Program I or Program II can derive the same band centers. However, as the right endpoint shifted to the right, in some cases Program I only found one line across both Band I and Band II (the red dashed line shown in Fig. 4). In this case, continuum removal using Program I derives a larger Band I center value and a smaller Band II center value than Program II. In general, Program II is recommended for continuum removal to acquire the band centers, because it finds the same Band I center with different right endpoints.

Table 1 shows the average difference between the band centers, which are derived using Point VII (2936 nm) as the right endpoint and using Point I (2457 nm) as the right endpoint. It can directly show the effect of shifting the right endpoint on the band centers derived using these two continuum removal programs. For the spectra using Program I to remove the continuum, the difference between the Band I centers varies from 1 to 5 nm, and the difference between the Band II centers varies from 74 to 92 nm. In contrast, for the spectra using Program II to remove the continuum, the difference between the Band I centers remains 0, and that between the Band II centers varies from 92 to 105 nm.

3.2 The Optimal Right Endpoint for Continuum Removal

Table 2 presents the average distance from the measurement position to the fitting curve, which uses the data for natural orthopyroxenes and clinopyroxenes (Adams 1974; Cloutis & Gaffey 1991) in the plot of Band II center versus Band I center (Fig. 5). Table 3 shows the order of these average distances in increasing order as the right endpoint shifted from Point I to Point VII. In Table 3, "1" is the nearest average distance, and "7" is the farthest distance. The optimal right endpoint for continuum removal is the wavelength with the shortest average distance (i.e., a value of "1" in Table 3).

Generally speaking, the optimal right endpoints for continuum removal mainly depend on different optical period data (OP1B and OP2A). For OP1B data, the optimal right endpoints appear at Point I (2457 nm) and Point II (2497 nm). For OP2A data, they are Point III (2537 nm) and Point IV (2576 nm). The region where the spectra were extracted also influenced the optimal right endpoint. The optimal right endpoints of the spectra extracted from Mare Humorum are a little larger (40 nm) than those of the spectra from Mare Nubium (Table 3), for both OP1B and OP2A data. The two continuum removal programs can derive the same optimal right endpoint. In general, for both programs, it is reasonable to set the right endpoints around 2480 and 2560 nm for OP1B and OP2A data, respectively.

3.3 Comparison Between OP1B and OP2A Data

Table 4 shows the average difference between the band center values derived from OP1B data and those derived from OP2A data. The Band I center values derived from OP1B data are smaller than those derived from OP2A data by about 9–12 nm. The Band II center values derived from OP1B data are slightly smaller (about 1–3 nm) than those derived from OP2A data when the right endpoints are close to 2500 nm. However, as the right endpoints shifted to longer wavelengths (> 2600 nm), the Band II center values derived from OP1B data become larger (about 1–14 nm) than those derived from OP2A data (Table 4).

As Figure 6 shows, the spectral slopes and band centers differ between OP1B and OP2A data. Table 5 presents the average spectral slopes in Band I and Band II, which use Point VI as the right endpoint. The spectral slopes of Band I and Band II are respectively represented by the slope of the straight line across Band I and Band II used in Program II (the green and yellow dashed lines shown in Figure 4). The spectral slopes of OP1B data are steeper than those of OP2A data in Band I but gentler in Band II (for the spectra using longer right endpoints) for most craters extracted from Mare Humorum and Mare Nubium. Generally speaking, the band center values derived from OP1B data are smaller than those derived from OP2A data in Band I but larger in Band II, which is possibly consistent with the fact that the spectral slopes of OP1B data are steeper than those of OP2A data in Band I but gentler in Band II.

Technically, the derived band centers should be independent of the spectral slopes after performing continuum removal. The continuum slope is consistent with the composition of a geologic material, whether it is mixed with another spectrally distinct geologic material, and the maturity or degree of space weathering experienced by the surface and the composition of the material. However, for spectra shown in Figure 6, the tangent points of the continuum around 1500 nm are different for OP1B and OP2A data. For OP1B data, the continuums have two independent tangent points around 1480 nm, while for OP2A data, the continuums have only one tangent point at 1508 nm. It is possible because the shape of the two spectra are different (different spectral slopes) which may be caused by uncertainties from instrumental artifacts. The optimized tangent point of the continuum removal program may cause the derived band centers to be different.

4 MINERALOGY OF MARE HUMORUM AND MARE NUBIUM

According to the above discussions, the optimal right endpoint for continuum removal is the key to derive the band centers that fit the trend of natural pyroxenes well in the plot of the Band II center versus the Band I center. Figure 7 shows the band centers of the craters extracted from Mare Humorum and Mare Nubium derived from the continuum removal using Program II. The right endpoints of these

Table 1 Average difference between the band centers, which were derived using Point VII (2936 nm) as the right endpoint and using Point I (2457 nm) as the right endpoint.

Average Difference	Location	Program I		Program II	
		OP1B	OP2A	OP1B	OP2A
Band I Center	Mare Humorum	3	5	0	0
	Mare Nubium	1	2	0	0
Band II Center	Mare Humorum	92	80	105	98
	Mare Nubium	92	74	99	92

Notes: These values were measured under Program I and Program II individually.

Table 2 The Average Distance from the Band Centers of Spectra to the Fitting Curve in the Band II Center versus Band I Center Plot

Data	Location	Program	Point I 2457 nm	Point II 2497 nm	Point III 2537 nm	Point IV 2576 nm	Point V 2616 nm	Point VI 2776 nm	Point VII 2936 nm
OP1B	Mare Humorum	I	8.32	7.10	8.20	10.73	13.18	17.33	18.28
		II	8.32	7.10	8.19	10.73	13.31	21.15	25.23
	Mare Nubium	I	7.54	8.24	10.61	13.49	16.16	22.34	24.20
		II	7.54	8.24	10.61	13.61	16.48	24.14	27.86
OP2A	Mare Humorum	I	14.04	11.15	9.62	9.15	9.25	10.53	10.55
		II	14.04	11.15	9.55	8.97	9.24	12.93	16.33
	Mare Nubium	I	12.89	10.83	9.87	9.90	10.68	12.61	13.03
		II	12.86	10.77	9.74	9.77	10.74	14.77	17.73

Notes: The curve was fitted with the data for natural orthopyroxenes and clinopyroxenes (Adams 1974; Cloutis & Gaffey 1991). An example is presented in Fig. 4.

Table 3 The sequence of the average distance, which is displayed in Table 2, as the right endpoint shifted from Point I to Point VII.

Data	Location	Program	Point I 2457 nm	Point II 2497 nm	Point III 2537 nm	Point IV 2576 nm	Point V 2616 nm	Point VI 2776 nm	Point VII 2936 nm
OP1B	Mare Humorum	I	3	1	2	4	5	6	7
		II	3	1	2	4	5	6	7
	Mare Nubium	I	1	2	3	4	5	6	7
		II	1	2	3	4	5	6	7
OP2A	Mare Humorum	I	7	6	3	1	2	4	5
		II	6	4	3	1	2	5	7
	Mare Nubium	I	6	4	1	2	3	5	7
		II	5	4	1	2	3	6	7

Notes: The order was determined by the average distance from near to far. "1" represents the nearest distance and "7" represents the farthest distance.

spectra are at the wavelengths with the shortest average distance in Table 3 (i.e., the wavelengths denoted with a value of "1") for the corresponding data. The band centers of natural pyroxenes, which are measured by Adams (1974) and modified by Cloutis & Gaffey (1991), and synthetic pyroxene data from Klima et al. (2011), are also plotted for comparison. As Figure 7 shows, for OP1B data, the band centers of Mare Humorum vary from 944 to 1001 nm in Band I and from 2016 to 2196 nm in Band II. The Band I and Band II centers of Mare Nubium are 923-1016 nm and 1957-2227 nm, respectively. For OP2A data, the band centers of Mare Humorum vary from 940 to 1015 nm in Band I and from 2057 to 2236 nm in Band II. The Band I and Band II centers of Mare Nubium are within 945-1017 nm and 1943-2223 nm, respectively. According to previous researches (Burns 1993; Cloutis & Gaffey 1991; Hazen et al. 1978; Klima et al. 2011), for orthopyroxene, which is low-Ca pyroxene, the Band I centers vary from 900 to 930 nm, and the Band II centers vary from 1800 to 2100 nm (Cloutis & Gaffey 1991). For high-Ca pyroxene, the Band I centers and the Band II centers range from 910 to 1070 nm and from 1970 to 2360 nm, respectively (Cloutis & Gaffey 1991). Comparing the performance of orthopyroxene and clinopyroxene, the pyroxene compositions of the spectra derived from Mare Humorum and Mare Nubium mostly display intermediate to high-Ca pyroxene features.

The distributions of OP1B and OP2A measurements are distinguishable in the plot of Band II center versus Band I center (Fig. 7). The scope of OP1B measurements is long and narrow, and the shape of OP2A measurements is shorter and wider. The boundary of the OP2A measurements tends to be on the upper-right side of the OP1B measurements along the fitting curve because the Band I center values derived from the OP2A data are generally larger than those derived from the OP1B data.

In the plot of BAR versus Band I center (Fig. 8), three silicate compositional groups are defined as OL, OC and BA (Gaffey et al. 1993), which are used to denote

Table 4 Average Difference between the Band Center Values Derived from the OP1B Data and Those Derived from the OP2A Data

Area	Program	Band Center	Point I 2457 nm	Point II 2497 nm	Point III 2537 nm	Point IV 2576 nm	Point V 2616 nm	Point VI 2776 nm	Point VII 2936 nm
Mare Humorum	I	I	–9.47	–9.47	–9.55	–9.74	–10.15	–11.08	–11.7
		II	–5.47	–3.44	–1.49	0.48	2.88	6.19	7.03
	II	I	–9.47	–9.47	–9.47	–9.47	–9.47	–9.47	–9.47
		II	–5.47	–3.44	–1.84	–0.67	0.17	1.3	1.55
Mare Nubium	I	I	–10.87	–10.88	–10.9	–10.98	–11.12	–12.04	–12
		II	–4.53	–1.75	0.34	1.69	3.06	8.35	14.12
	II	I	–10.86	–10.86	–10.86	–10.86	–10.86	–10.86	–10.86
		II	–4.61	–1.9	0.07	1.11	1.91	4.01	3.06

Table 5 Average Slopes of the Spectra

Optical Period	Band I [a]		Band II (2776 nm) [b]	
Data	Mare Humorum	Mare Nubium	Mare Humorum	Mare Nubium
OP1B (10^{-5})	2.745	3.187	3.059	3.115
OP2A (10^{-5})	2.568	2.702	3.348	3.118

Notes: [a]- The spectral slope is represented by the slope of the straight line across Band I in Program II (the green dashed line in Fig. 4). [b]- The spectral slope is represented by the slope of the straight line across Band II in Program II (the yellow dashed line in Fig. 4). These spectra used Point VI (2776 nm) as the right endpoint.

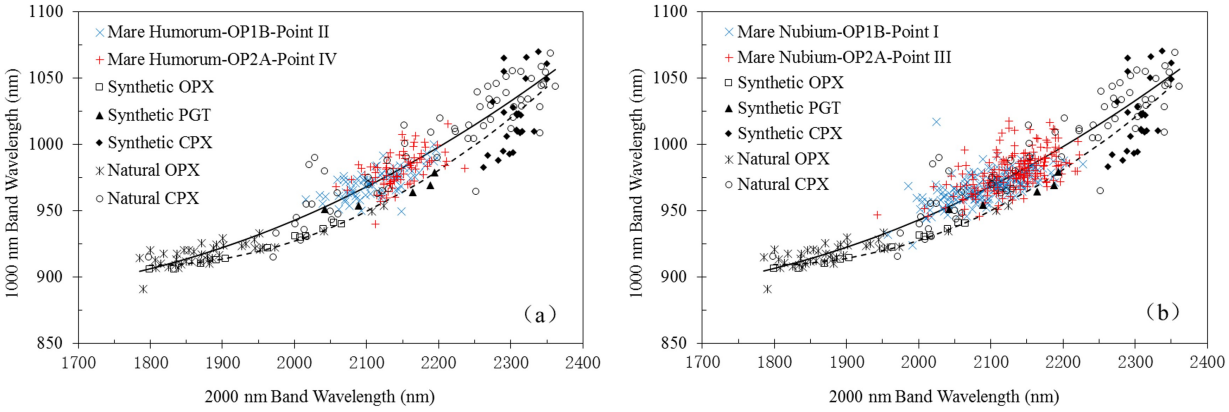

Fig. 7 Plot of Band II center versus Band I center. The spectra were extracted from Mare Humorum and Mare Nubium using Program II for continuum removal. For comparison, the band centers of natural pyroxenes measured by Adams (1974) and modified by Cloutis & Gaffey (1991) are shown. Synthetic pyroxene data from Klima et al. (2011) are also plotted. The black solid line represents the fitting curve of natural pyroxenes. The black dashed line represents the fitting curve of synthetic pyroxenes. (a) The blue crosses show the OP1B data of Mare Humorum (the right endpoint at Point II). The red crosses show the OP2A data of Mare Humorum (the right endpoint at Point IV). (b) The blue crosses show the OP1B data of Mare Nubium (the right endpoint at Point I). The red crosses show the OP2A data of Mare Nubium (the right endpoint at Point III). OPX means orthopyroxene, CPX means clinopyroxene and PGT means pigeonite.

monomineralic olivine assemblages, mafic silicate components of ordinary chondrites, and pyroxene-dominated basaltic achondrite, respectively. Some subgroups are also drawn for comparison, which represent the different relative content of olivine and pyroxene. Most measurements of the fresh craters extracted from Mare Humorum and Mare Nubium fall into the region above the OC area, for both OP1B and OP2A data, which probably indicates the olivine-clinopyroxene mixtures. Few measurements of Mare Nubium are within the BA area, which may represent the pyroxene (i.e. orthopyroxene) dominated composition. Generally speaking, relative content (olivine/pyroxene) of the fresh craters extracted from Mare Humorum and Mare Nubium seem to approximately range from the olivine-clinopyroxene mixtures to orthopyroxene dominated composition, for both OP1B and OP2A data, which confirms that the craters extracted from Mare Humorum and Mare Nubium are suitable for studying the optimal right endpoint of M^3 data by comparing the band centers of natural pyroxenes.

In addition, for both Mare Humorum and Mare Nubium, more scattered points of OP1B data are in the OC region than those of OP2A data because the Band I center values of OP2A data are usually larger than those of OP1B data, which increases the height of the positions of these measurements in this plot. Craters rich in olivine like

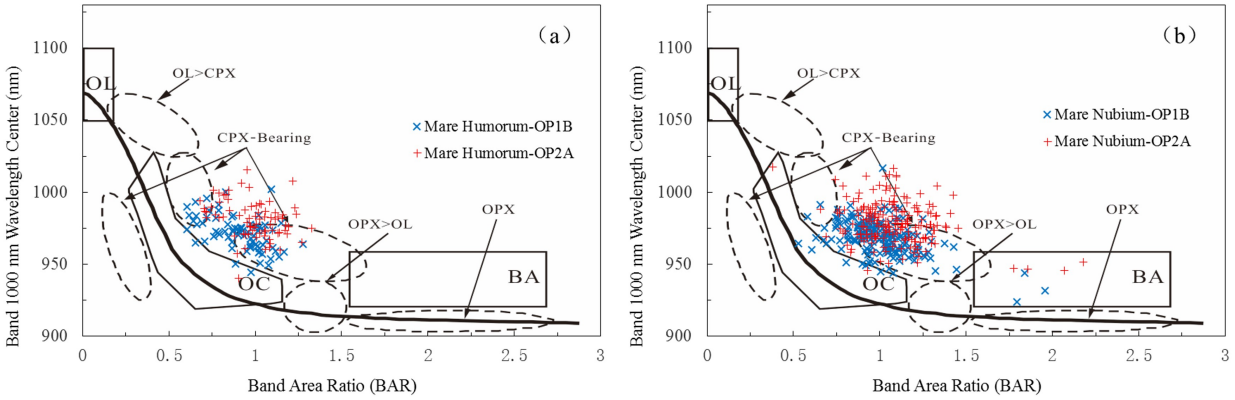

Fig. 8 Plot of BAR versus Band I center. The spectra were input to Program II for continuum removal using Point II (2497 nm) for the right endpoint. Three polygons from Gaffey et al. (1993) are drawn on this plot. Various subgroups are also presented for comparison. The black solid line indicates the location of the olivine-orthopyroxene mixing line (Cloutis et al. 1986). (a) The blue crosses show the OP1B data of Mare Humorum. The red crosses show the OP2A data of Mare Humorum. (b) The blue crosses show the OP1B data of Mare Nubium. The red crosses show the OP2A data of Mare Nubium.

the Eratosthenian basalts in Mare Imbrium (e.g., Wu et al. 2015) were not found in this study.

5 CONCLUSIONS

This paper explored the continuum removal method and compared the difference for both OP1B and OP2A M^3 data. Generally, the optimal right endpoint for continuum removal varies with the M^3 optical period data. The optimal right endpoints are around 2480 and 2560 nm for OP1B and OP2A data, respectively. The band center values derived from Program I for continuum removal are larger than those derived from Program II in Band I but smaller in Band II. Program II is recommended for calculating the band centers because it can give the same Band I center with different right endpoints. The Band I center values derived from OP1B data are smaller than those derived from OP2A data because most spectral slopes of OP1B data are steeper than those of OP2A data in Band I. The Band II center values derived from OP1B data are smaller than those derived from OP2A data when the right endpoints are close to 2500 nm. However, as the right endpoints shifted to longer wavelengths ($>$ 2600 nm), the Band II center values derived from OP1B data become larger. It is possible that most spectral slopes of OP1B data are gentler than those derived from the OP2A data in Band II for the spectra using longer right endpoints. This result is consistent with the results from Wu et al. (2015), where different spectral slopes between OP1B and OP2A data influence the variation of the band centers, which confirms the reliability of our research. In the plot of Band II center versus Band I center, the distribution boundary of the OP2A measurements is on the upper-right side of the OP1B measurements. The pyroxene compositions of the craters extracted from Mare Humorum and Mare Nubium display intermediate to high-Ca pyroxenes features. In the BAR versus Band I center plot, the relative content (olivine/pyroxene) of most craters extracted from Mare Humorum and Mare Nubium appears to range from the olivine-clinopyroxene mixtures to orthopyroxene-dominated composition.

A reliable method to estimate spectral parameters from M^3 data is significant for mineral identification. By analyzing for large amounts of craters and multiple optical period data, this study provided a more precise method to use M^3 data and to aid future work. Considering that the study of the continuum removal method was only applied to Mare Humorum and Mare Nubium, but the spectra of highland materials have not been compared in this paper, more samples and different areas of the Moon should be studied in further work.

Acknowledgements This study was supported by the Macau Science and Technology Development Fund (048/2012/A2, 091/2013/A3 and 039/2013/A2), the National High Technology Research and Development Program of China (863 Program, 2015AA123704) and the National Natural Science Foundation of China (Nos. 41172296 and 41422110).

References

Adams, J. B. 1974, J. Geophys. Res., 79, 4829

Adams, J. B. 1975, Interpretation of Visible and Near-infrared Diffuse Reflectance Spectra of Pyroxenes and Other Rock-forming Minerals, Infrared and Raman Spectroscopy of Lunar and Terrestrial Minerals (Academic Press New York), 91

Boardman, J. W., Pieters, C. M., Green, R. O., et al. 2011, Journal of Geophysical Research (Planets), 116, E00G14

Burns, R. G. 1993, Mineralogical Applications of Crystal Field Theory, ed. Roger G. Burns (Cambridge, UK: Cambridge Univ. Press), 575

Clark, R. N., Pieters, C. M., Green, R. O., Boardman, J. W., & Petro, N. E. 2011, Journal of Geophysical Research (Planets), 116, E00G16

Clark, R. N., & Roush, T. L. 1984, J. Geophys. Res., 89, 6329

Cloutis, E. A. 1985, Interpretive Techniques for Reflectance Spectra of Mafic Silicates, PhD thesis (University of Hawaii at Manoa)

Cloutis, E. A., Gaffey, M. J., Jackowski, T. L., & Reed, K. L. 1986, J. Geophys. Res., 91, 11641

Cloutis, E. A., & Gaffey, M. J. 1991, J. Geophys. Res., 96, 22809

Crown, D. A., & Pieters, C. M. 1987, ICARUS, 72, 492

Gaffey, M. J., Burbine, T. H., Piatek, J. L., et al. 1993, ICARUS, 106, 573

Green, R. O., Pieters, C., Mouroulis, P., et al. 2011, Journal of Geophysical Research (Planets), 116, E00G19

Hazen, R. M., Bell, P. M., & Mao, H. K. 1978, in Lunar and Planetary Science Conference Proceedings, 9, 2919

Hiesinger, H., Jaumann, R., Neukam, G., & Head, J. W. 2000, J. Geophys. Res., 105, 29239

Hiesinger, H., Head, J. W., Wolf, U., Jaumann, R., & Neukum, G. 2003, Journal of Geophysical Research (Planets), 108, 5065

Isaacson, P. J., Petro, N. E., Pieters, C. M., et al. 2012, in Lunar and Planetary Science Conference, 43, 1740

Klima, R. L., Pieters, C. M., & Dyar, M. D. 2007, Meteoritics and Planetary Science, 42, 235

Klima, R. L., Pieters, C. M., Boardman, J. W., et al. 2011, Journal of Geophysical Research (Planets), 116, E00G06

Kusuma, K. N., Sebastian, N., & Murty, S. V. S. 2012, Planet. Space Sci., 67, 46

Lucey, P. G. 2004, Geophys. Res. Lett., 31, L08701

McCord, T. B., & Adams, J. B. 1973, Moon, 7, 453

Pieters, C. M. 1978, in Lunar and Planetary Science Conference Proceedings, 9, 2825

Pieters, C. M., Head, J. W., Whitford-Stark, J. L., et al. 1980, J. Geophys. Res., 85, 3913

Pieters, C. M., Taylor, L. A., Noble, S. K., et al. 2000, Meteoritics and Planetary Science, 35, 1101

Pieters, C. M., Boardman, J., Buratti, B., et al. 2009, Curr. Sci, 96, 500

Staid, M. I., & Pieters, C. M. 2001, J. Geophys. Res., 106, 27887

Staid, M. I., Pieters, C. M., Besse, S., et al. 2011, Journal of Geophysical Research (Planets), 116, E00G10

Varatharajan, I., Srivastava, N., & Murty, S. V. S. 2014, ICARUS, 236, 56

Wu, Y. Z., et al. 2015, Geology, Tectonism and Composition of the Northwest Imbrium Region, Icarus: LRO Special Issue, submitted